Journal of Applied Electrochemistry **31**: 1381–1387, 2001.

Electrochemical chromic acid regeneration process with fuel-cell electrode assistance. Part I: Removal of contaminants

M.I. AHMED, T.M. HOLSEN† and J.R. SELMAN*
Department of Chemical and Environmental Engineering, Illinois Institute of Technology, Chicago, IL 60616, USA
†Present address: Civil and Environmental Engineering Department, Clarkson University, Potsdam, NY 13699, USA
*(*author for correspondence)*

Received 22 December 2000; accepted in revised form 17 August 2001

Abstract

This paper presents the results of work carried out on a laboratory cell for regeneration of spent hard chrome plating solution. The electrolysis cell consists of a rectangular tank divided into two compartments with an ion exchange membrane (Nafion-117), and uses a lead anode and a gas diffusion electrode as the cathode. The laboratory scale cell was used as a simulated plating bath containing Cu^{2+}, Fe^{2+}, Ni^{2+}, and Cr^{3+} as contaminants, for different experimental conditions at room temperature. The separation performance of the process was assessed by operating the cell under three constant current conditions. The cell was also tested under different initial concentrations and catholyte-to-anolyte volume ratios. The results indicate the possibility of decreased energy consumption and better removal rates over traditional methods.

1. Introduction

In the hard chrome plating industry, acid chromate ($Cr_2O_7^{2-}$) plating baths become contaminated by Cu^{2+}, Fe^{2+}, and Ni^{2+} ions through corrosion of metal accessories, and by Cr^{3+} ions as a result of $Cr_2O_7^{2-}$ reduction. These contaminants degrade the quality of hard chrome deposit [1]. For example, high concentrations of Cr^{3+} in the plating bath cause surface roughness of the deposit and reduce current efficiency. It is therefore desirable to continuously remove them from the plating bath to avoid the expense and legal liability of the disposal process.

Previous work using a laboratory-scale porous ceramic membrane (PCM) cell [2], has confirmed that impurities such as Ni, Fe and Cu ions present in hard chromium plating solution can be removed and concentrated as a metal hydroxide sludge by operating a parallel, 'in-tank', small-scale electrolysis process. This process uses a PCM that is suspended in the plating bath. A lead cathode is placed inside the diaphragm cell, which is surrounded by a perforated oxide-coated lead anode. During the operation of the PCM, metals are drawn into the cell and trivalent chromium in the bath is oxidized to hexavalent chromium at the outer lead anode. This type of PCM has been used in the plating industry since the 1840s and can be classified as electrolytic [3].

In laboratory experiments with the PCM process [2, 4, 5], it was found that frequent cleaning was required as the cathode became coated with metals, the pores of the ceramic diaphragm were clogged with insoluble metal hydroxides, and sludge accumulated in the pot when sulfuric acid is used as the catholyte. However, when chromic acid is used as the catholyte, no sludge formation is observed [6, 7]. In addition, the power requirements were fairly high, particularly when the cathode was coated with metals and the pores became clogged. Therefore, it is attractive to explore alternatives or improvements to the PCM process.

Other, more sophisticated processes have been developed. GM's process with a Nafion separator and lead electrodes showed good efficiency in trivalent chrome reoxidation [8]. In 1980 the Bureau of Mines [9] demonstrated a flow-through system for the regeneration of chromic acid composed of a copper cathode, a lead anode, and a Nafion separator. However, these processes lack operational spontaneity and cost effectiveness. In this work a compatible process is developed to improve the efficiency and energy consumption characteristics of hard chrome plating solution regeneration processes using a Nafion membrane and an oxygen-reducing cathode (fuel cell oxygen cathode).

2. Experimental

2.1. *Experimental cell*

The laboratory-scale cell was designed and fabricated using a rectangular piece of Nafion-117 (Figure 1), with a projected active area of 40 cm^2, and a volume of 1.2 dm^{-3}. The fuel cell cathode assembly (Figure 2)

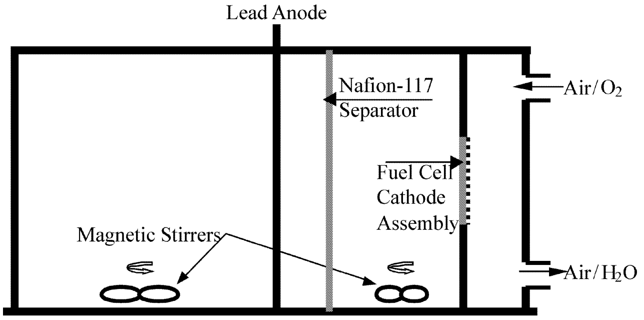

Fig. 1. Schematic of experimental cell. Anode projected area 100 cm^2, cathode projected area 5 cm^2, with 5 mg cm^{-2} Pt-black loading, separator 7.5 × 12.5 cm (40 cm^2 used), and the utilized volume of cell 1.2 dm^{-3}. Hg/$HgSO_4$ reference electrode.

consists of a so-called membrane–electrode-assembly (MEA), a gas diffusion backing layer, and a flow distributor. The MEA includes a Nafion membrane that contacts the electrolyte of projected area 5 cm^2. On the gas side it contacts a porous non-catalytic conductor (carbon cloth) that acts as a gas diffuser. A noble metal catalytic layer embedded in the Nafion surface contacts the Nafion as well as the carbon conductor. A new MEA, manufactured at IIT, was used in each experiment. It was fabricated based on methods developed by Wilson et al. [10, 11]. The catalytic surface is supplied with the oxidant gas (usually air) via the carbon cloth and the flow distributor. The latter is a graphite block with a suitable flow field machined into it, which optimizes access of gas to the backside of the MEA. The unmodified Nafion surface faces the interior of the cell.

The anode of the cell is a lead plate of 100-cm^2 projected area, placed in the anolyte compartment. Passage of current drives metal cations through the Nafion membrane towards the catholyte, in preference to chromate ions. Before use, the lead anode was passivated by passing a positive current (mA) in a sulfuric acid solution for 2–4 h at a constant electrode potential of 0.4 V.

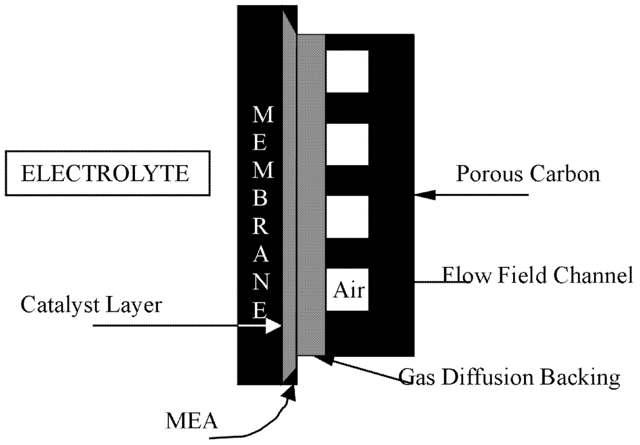

Fig. 2. Details of the fuel cell cathode assembly, including MEA, gas diffusion backing layer, and flow distribution plate.

Replacing hydrogen evolution by oxygen reduction reduces the theoretical (thermodynamic) standard cell voltage by 1.23 V at 25 °C. However, the actual savings in cell voltage will be less, depending on kinetics and mass transfer losses, as well as the reduced activity of O_2 in air. Also, when these voltage savings are translated into cost savings, the price of pressurized air (at slight overpressure) and the cost of the fuel cell cathode assembly in relation to a lead electrode must be taken into account.

In preliminary experiments, overheating of the fuel cell cathode assembly led to its disintegration and damaged the Nafion-117 membrane. Therefore, different materials and configurations for the fuel cell oxygen cathode were tested. Overheating was overcome by replacing the backing material with platinum gauze to improve electronic conductivity, maximize oxygen diffusion into the electrode, and facilitate water removal from it.

2.2. *Procedure*

All experiments were carried out in simulated spent chrome plating solution similar to the one found in plating practice. It had a chromic acid concentration of 250 g dm^{-3} and contained Cr^{3+}, Cu^{2+}, Fe^{2+} and Ni^{2+} as impurities [12, 13]. The impurities were added to the chromic acid in the form of sulfates ($FeSO_4 \cdot 7H_2O$, $CuSO_4$, $NiSO_4 \cdot 6H_2O$ and $Cr_2(SO_4)_3 \cdot 12H_2O$) to achieve impurity concentrations in the desired range (typically 0.1 M). Barium carbonate ($BaCO_3$) was used to eliminate excess sulfate anion by the formation of a water-insoluble precipitate ($BaSO_4$). Filters were used to separate the $BaSO_4$ precipitate from the plating solution.

The following operating parameters were systematically varied: applied current (0.2, 0.4, 0.6 A), initial contaminant concentrations (high, low) and the catholyte-to-anolyte-volume ratio (1/3, 1/6). Also the cathode gas environment was varied (air, argon), to assess energy savings. Samples were taken to determine the composition of the anolyte and catholyte. Cu, Ni, and Fe concentrations were determined using flame-atomic adsorption spectrometry (AAS). Trivalent and hexavalent chromium concentrations were determined using titration [2].

3. Chromic acid regeneration and metal impurity removal

3.1. *Results*

Experiments were conducted to determine the effect of current, initial concentration and volume ratio on transport rates of impurities from the anolyte (representing the main plating bath) into the catholyte compartment or concentration cell. The initial concentrations in both compartments were the same, to initially eliminate diffusion as a driving force to transport ions through the membrane.

In preliminary experiments a pure platinum anode was used to ensure inertness. In subsequent experiments a Pb anode was used. One of the differences in these experiments is that when an acidic solution of chromic acid salt is electrolyzed with a pure platinum electrode, the principal anode product is oxygen, whereas if a lead electrode is used, almost quantitative production of dichromate results [14] in addition to oxygen evolution. This reaction mechanism involves the oxidation of lead to PbO_2 (which is a catalyst for Cr^{3+} oxidation). This catalysis is advantageous in reducing Cr^{3+} concentrations, although this process increases resistivity because lead oxide is poorly conductive. The capital cost of a lead anode is much smaller than platinum and many other potential anodes therefore it is the sole anode material used in the hard chrome electroplating industry.

The time variation of Cr(VI) and Cr(III) concentrations in the anolyte at various operating currents (0.2, 0.4, 0.6 A), initial contaminant concentrations (low: 90, 106, 107, 112 mmol dm^{-3}; high: 110, 128, 145, 165 mmol dm^{-3} for Cr^{3+}, Cu, Fe, and Ni respectively), and in an oxygen-free environment (argon purged solution), are shown in Figure 3a. The corresponding catholyte concentrations are shown in Figure 3b. These results confirm that Cr^{3+} is rapidly oxidized under these conditions as has been reported in the literature for a similar process [8] (the type of membrane and cathode used in that process were not reported). In that process [8] trivalent chrome reoxidation is very efficient, so that the rate of Cr^{3+} reoxidation is largely equal to the rate of Cr^{3+} production. In the present work this transport rate from the catholyte (as a result of chromate reduction at the cathode) to the anolyte tends to become very low.

Metallic impurity (Fe, Ni, and Cu) concentrations during operation at 0.2 A and 1/3 catholyte-to-anolyte-volume ratio are shown in Figure 4. A summary of the removal rates based on linear regression of all experimental data is shown in Table 1 together with the corresponding correlation coefficients with respect to time. The removal rates were normalized with respect to the initial concentration of each impurity. The amount of metal impurity plated onto the cathode during each experiment was calculated from the mass balance (Table 2) (X-ray diffraction analysis of the cathode revealed that metals are being plated onto the cathode (M.I. Ahmed et al., submitted for publication)).

3.2. *Discussion*

3.2.1. *Trivalent chrome reoxidation and hexavalent chrome leakage*

In this low pH range the dominant mechanisms for trivalent chrome reoxidation is [15],

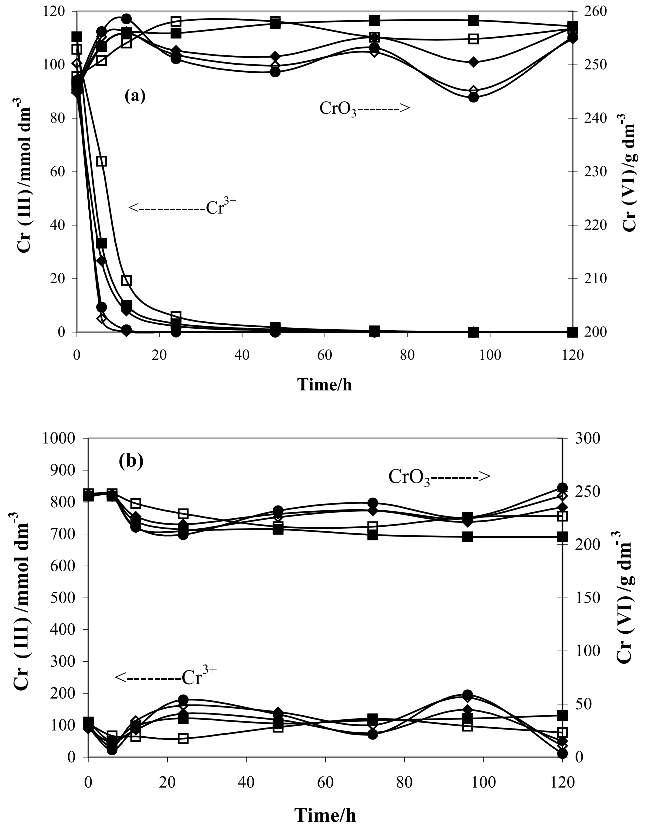

Fig. 3. Trivalent (Cr^{3+}) and hexavalent (as CrO_3) chromium concentrations in the anolyte (a) and catholyte (b). Low-0.2 A (◆), high-0.2 A (■), argon-0.2 A (□), low-0.4 A (●), low-0.6 A (◇).

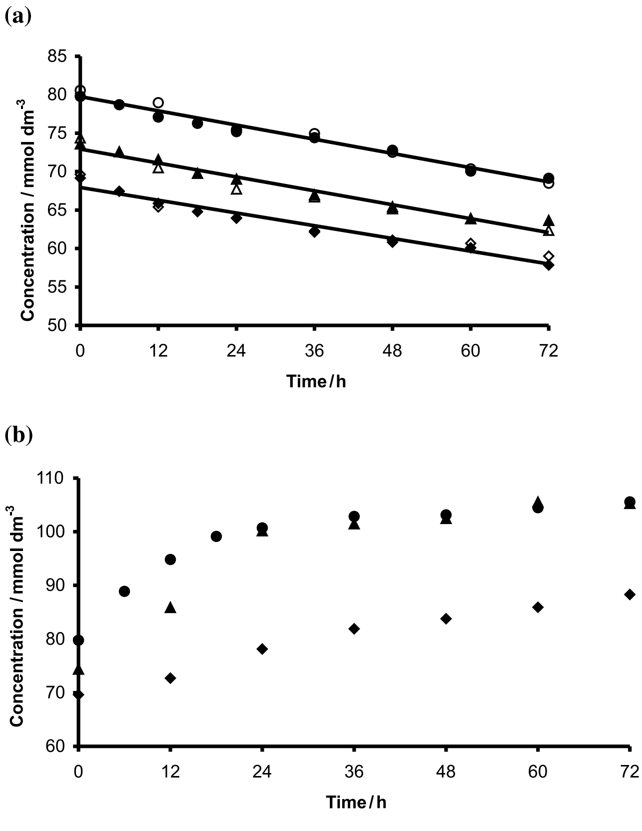

Fig. 4. Impurity concentrations in the anolyte (a) and catholyte (b) operating at 0.2 A Cu (◆), Fe (●), Ni (▲).

Table 1. Impurity removal rates from the anolyte based on a linear fit

Current (A)	Removal rates (mmol dm^{-3} d^{-1}), normalized metal removal rate (d^{-1}) and correlation coefficients (r^2)			
	Duration (h)	Cu	Fe	Ni
0.2 [1/3 V_c/V_a]	72	3.310 0.047 (0.92)	3.691 0.053 (0.95)	3.691 0.050 (0.98)
0.4 [1/3 V_c/V_a]	120	6.346 0.060 (0.99)	5.866 0.055 (0.99)	5.906 0.053 (0.99)
0.6 [1/3 V_c/V_a]	120	6.902 0.071 (0.99)	6.430 0.065 (0.99)	7.524 0.069 (0.98)
0.4 [high concentration]	120	6.799 0.053 (0.98)	7.210 0.049 (0.90)	8.407 0.051 (0.92)
0.2 [1/6 V_c/V_a]	120	1.906 0.023 (0.88)	4.394 0.044 (0.79)	2.962 0.032 (0.72)

$$\begin{gathered}\mathrm{Cr^{3+} + 4\,H_2O \longleftrightarrow H_2CrO_4 + 6\,H^+ + 3\,e^-} \\ E^0 = 1.335\text{–}0.1182\ \mathrm{pH} + 0.0197\ \log\frac{\{\mathrm{H_2CrO_4}\}}{\{\mathrm{Cr^{3+}}\}} \qquad (1)\end{gathered}$$

This reoxidation reaction consumes water and produces protons, thereby keeping the solution at very low pH. This loss of water, in addition to losses by evaporation and electrolysis, was compensated for in these experiments by adding H_2O to maintain a constant volume. These intermittent additions are at least partly responsible for the oscillations in concentrations shown in Figure 3.

3.2.2. *Metallic impurity removal*

Three-dimensional porous electrodes are capable of operating at high current densities (based on projected area), thus, increasing removal efficiencies while maintaining stable currents.

Based on an average Pt particle size of 2.2 nm, the electroactive Pt surface area (EPSA) is 128 m^2 g^{-1} [16, 17]. For an 80% Pt/C electrode, Electrochem Inc (A. Arkins, private communication) reports a total electroactive area of 140 m^2 g^{-1} Pt-black. When passing 0.2 A total current, the projected current density at the cathode is 0.04 A cm^{-2}, so the current density relative to carbon area is 2.9×10^{-5} A cm^{-2}, that relative to active Pt area is 7.1×10^{-6} A cm^{-2}, and that relative to total active area is 5.7×10^{-6} A cm^{-2}.

The contaminant removal rates at such low current densities are probably not mass-transfer limited, nor do they show dependence on plating potentials of the individual metallic species. The removal rates depend on the strength of the electrical field due to the major ohmic resistance provided by Nafion-117 membrane, thereby making the process a quasi-steady state process. This yields the approximately linear profiles for removal from the anolyte shown in Figure 4a. As seen from Table 1, the correlation coefficient is quite strong, and indicates, for example, in the case of copper at 0.2 A, that 92.3% of the anolyte concentration time-variation is explained by a linear relationship [18].

The good correlation coefficients indicate constant selectivity of the process, with respect to metal impurities. The higher values of correlation coefficients obtained at higher applied currents (Table 1), confirm this constant selectivity. The larger proportion of metal deposition at high current (Table 2) does not contradict this conclusion.

The normalized removal rates (r/C_0) of the three cations in each experiment are similar (for example, 0.047, 0.053, 0.050 d^{-1} for Cu, Fe, Ni respectively at 0.2 A) indicating that the removal rate depends primarily on the initial ion concentration. These rates generally increase slightly at higher currents. This dependence is also evident from the initial slopes (first day) of experiments carried out at higher currents and higher initial concentrations compared to the experiment carried at 0.2 A. The initial slopes are steeper in the former case, due to higher applied current as well as higher initial concentration, as will be explained in the following discussion. For example a remarkable increase in the removal rates was obtained at 0.4 and 0.6 A (Table 1), however this increase is not proportional to the increase

Table 2. Amount of specific impurity plated onto the cathode during operation at various current densities, and the percentage of the amount removed which is plated out

Current (A)	Metal plated out (mmol) and fraction plated (%)			
	Duration (h)	Cu	Fe	Ni
0.2 [1/3 V_c/V_a]	72	4.26 ± 0.42 43	1.75 ± 0.13 17	1.43 ± 0.16 14
0.4 [1/3 V_c/V_a]	120	26.96 ± 0.26 95	18.85 ± 2.71 72	23.54 ± 2.46 91
0.6 [1/3 V_c/V_a]	120	24.45 ± 1.35 78	23.74 ± 0.05 80	28.43 ± 3.05 82
0.4 [high concentration]	120	29.50 ± 0.33 91	27.95 ± 1.18 84	37.78 ± 0.28 93
0.2 [1/6 V_c/V_a]	120	2.42 ± 1.28 40	8.61 ± 2.01 62	4.46 ± 4.34 44

in the total applied current. At higher total currents, plating increased, probably due to increased concentrations of impurities in the catholyte (Table 2). In general, removal rates at 0.2 and 0.4 A were in the order Fe > Ni > Cu, and at 0.6 A Ni < Fe < Cu. Only in the latter case does the order conform to the standard plating potentials of the species considered.

Evidence from initial experiments in which low initial concentrations of copper compared to nickel and iron were used indicated that the initial concentration of the impurities plays a role in their removal rates. Hence, experiments were conducted at higher initial concentrations. In these experiments initial removal rates were faster (11.8, 18.0, 20.7 mmol dm^{-3} d^{-1} in the high concentration case compared to 6.3, 5.9, 5.9 mmol dm^{-3} d^{-1} in the low concentration case for Cu, Fe, Ni respectively, based on first day calculations), however, the overall reduction in impurity concentration after 120 h is approximately the same as in the low concentration case (Table 1).

Because a concurrent objective of these experiments was to quantify energy savings, removal rates when operating with argon as the cathode gas in an argon purged solution (no oxygen) were compared with the standard cathode gas, i.e., air. It was evident that removal rates are not significantly affected by shifting from oxygen reduction to hydrogen evolution potential, possibly due to the high electrode surface area. The metal deposition that occurs during operation might partially deactivate the electrode, however it does not completely inhibit gas evolution or water formation. Thus, observations from these experiments lead to an important conclusion, which is the fuel cell oxygen electrode is very durable with respect to deactivation.

The inter-electrode gap, electrode–separator distance, and catholyte-to-anolyte ratio (including membrane area to bath volume ratio) play an important role in process efficiency and power consumption. Migration of positively charged impurities from the anolyte to catholyte during electrolysis causes the concentration profile to a maximum at the negative electrode (cathode) and a minimum at the positive electrode (anode). Without plating, a back-diffusion potential develops counteracting the migration or electric potential. This back-diffusion potential is obviously dependent on the volume of the catholyte, or the catholyte-to-anolyte-volume ratio. In our experiments, three volume ratios were tested $(V_c/V_a) = \frac{1}{3}, \frac{1}{6}, \frac{1}{12}$, operating at 0.2 A. In the latter case, no significant removal was observed confirming that back diffusion was occurring. Operating at 0.2 A and $\frac{1}{6}$ volume ratio at a total volume of 1.2 dm^3 also reduced the removal rates significantly. Since a process objective is reduce the source of chromium disposal, operating at the smallest achievable volume ratio is important, and apparently this is a compromise between disposal volume, environmental regulations, cost of energy, and electrode exhaustion.

4. Energy consumption and efficiency

Figure 5 shows the cell voltage required to sustain the operation at 0.2, 0.4, 0.6 A. The cell voltage is obviously dependent on the applied current and initial concentration. The cell voltage during electrolysis at 0.4 A with a higher initial concentration is less than in the low concentration case. However, in all cases, the cell voltage increases with time indicating increased cell resistance. The most important feature in Figure 5a is the potential energy saving of at least 1 V obtained by supplying oxygen to the cathode leading to water production.

4.1. *Efficiency*

To achieve separation, the cathode must be driven towards negative potentials so that it will attract cations and the anode towards more positive potentials so that it will attract anions. This movement of cations to the cathode and anions to the anode (separation) is affected by the ionic current in the electrolyte, which is, in turn, completed by an externally applied and controlled electronic current in the outer electric circuit. Operating at a controlled current, or even at controlled voltage, leaves the cathode potential uncontrolled. This, in turn,

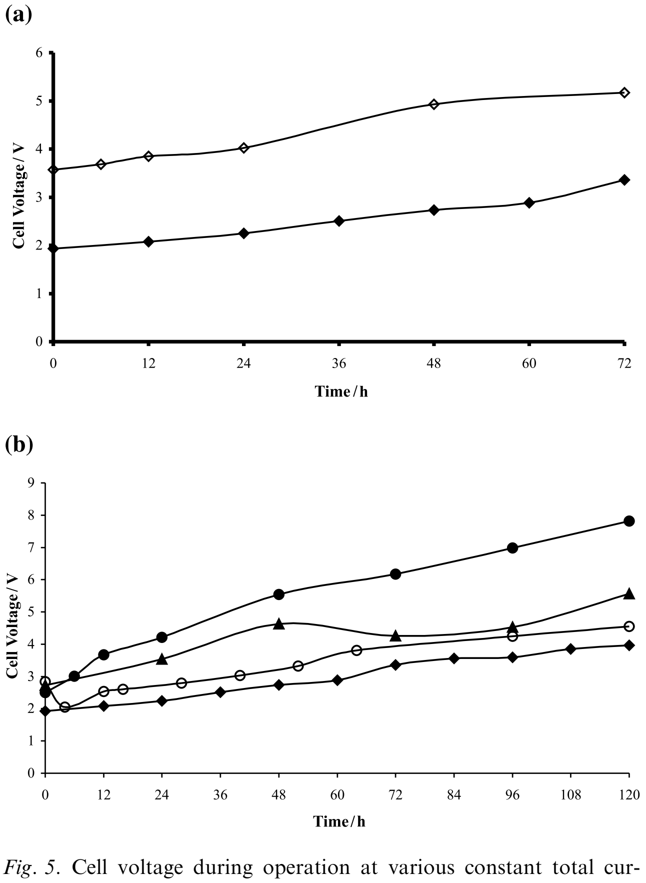

Fig. 5. Cell voltage during operation at various constant total currents. Comparison between air/oxygen supplied cathode and argon purged conditions (a) during removal experiments at various currents (b). (a) 0.2 A argon (◇), 0.2 A, air/O_2 (◆). (b) 0.2 A (◆), 0.4 A (▲), 0.4 A high concentration (○), 0.6 A (●).

Table 3. Efficiency during operation at various currents

Current (A)	Experiment duration (h)	Current (mA, Equation 1)				Energy consumption (kJ dm^{-3} mol^{-1})
		Cu	Fe	Ni	Efficiency (%)	
0.2	72	6.65	7.42	7.28	10.675	4127
0.4	120	12.76	11.79	11.87	9.105	8030
0.6	120	13.87	13.01	15.12	7.002	13723
0.4 (high)	120	13.67	14.49	16.90	11.265	5397
0.2 (1/6 V_c/V_a)	120	4.38	10.10	6.80	10.640	–

may cause the cathode potential to shift towards the reduction potential of species other than oxygen. Therefore, the oxygen reduction efficiency, which is high on platinum electrodes, but controlled by oxygen availability, water drainage properties of the electrode, temperature, and pH, may be less than optimal. For maximum efficiency of the process the cathode potential must be in the range where protons are adsorbed, however, metal cations may be adsorbed as well, leading to their deposition by electron transfer. This is an issue of compromise between long term stability of the electrode and process efficiency.

The low removal efficiency of the process was not due to the poor performance of the cell, rather; it was due to the transport resistance through Nafion-117 membrane at the cathode surface and the separator (M.I. Ahmed et al., submitted for publication). This is in addition to the high transference number of protons through Nafion-117.

The current used to transport the impurity across the Nafion-117 membrane was calculated from the following equation [19]

$$i = F \sum_i z_i N_i \tag{2}$$

Here N_i mol cm^{-2} s^{-1}, is the flux of species i, and z_i is the number of charges of the ion.

The efficiency was calculated by dividing the total current due to transport of Cu, Fe, and Ni by the total passed current. The current calculated from Equation 2, the efficiency, and energy consumption per total moles per cubic decimeter of Cu, Fe, Ni removed are shown in Table 3.

The efficiency decreases with increasing applied current, however, increasing the initial concentration by 50% increased the efficiency by 25% in the 0.4 A case. Yet the least energy consumption was obtained at 0.2 A. Thus, operating at higher currents such as 0.4 A in the high concentration case is similar to operation at low current density (0.2 A) with low concentration of impurity.

5. Conclusions

The feasibility of chromic acid regeneration using the designed cell was demonstrated. It was found that the process metallic impurity removal is slow compared to trivalent chrome reoxidation at the anode, which disappeared completely in about 2 days. Also the removal rates increase as the applied current is increased, and the higher the initial concentration the higher the removal rates, indicating the impurity removal rates are controlled by constant resistance (Nafion-117).

Supplying oxygen to the cathode has no significant effect on removal rates, however, reduction in the cell voltage results. Also operation at very low current density is dependent on the selectivity of the Nafion-117 membrane, and at higher currents the deposition of metals dominates the overall removal. In addition, operation at low current densities yields high efficiency and minimum energy consumption. However, there is no practical difference between cleaning the solution with low impurity concentration at 0.2 A, or waiting for higher impurity concentration and cleaning at 0.4 A.

Acknowledgements

The authors would like to thank the EPA (project no. R 82-7125-01-0) and Dr S. Balakrishnan project officer for their support in this study.

References

1. N.V. Mandich, Removal of metallic impurities in chromium plating solutions by porous pot method. In *Chromium Colloquium*, AESF, Orlando, FL, 1994 pp. 51–62.
2. C.C. Li, Removal of metal impurities from chromic acid solution by a ceramic diaphragm. Masters Thesis, Illinois Institute of Technology, Chicago, IL (1995).
3. G.C. Cushnie and W. Anderson, Removal of metal cations in chromium plating solution. In *Proceedings of AESF/EPA Hard Chromium Plating Workshop*, Orlando, FL, 1989 pp. 21–27.
4. S.L. Guddati, T.M. Holsen, C.C. Li, J.R. Selman and N.V. Mandich, *J. Appl. Electrochem* **29** (1999) 1129.
5. N.V. Mandich, C.C. Li and J.R. Selman, *Plating Surf. Finishing* **84** (1997) 82.
6. J. Pattanyak, N.V. Mandich, K. Mondal, T. Wiltowski and S.B. Lalvani, *Environ. Technol* **20** (1999) 317.
7. J. Pattanyak, N.V. Mandich, K. Mondal, T. Wiltowski and S.B. Lalvani, *Metal Finishing* (2000) 39.
8. K.N.G. Patrick and D.S. Dexter, *J. Mem. Sci.* **13** (1983) 327.
9. B. Kippling, General applications of perfluorinated ionomer membranes. In *Perfluorinated Ionomer Membranes*, *ACS Symposium Series,* A. Eisenberg and H. Yeager (ed.), Vol. 180, 1982, p. 475.

10. M.S. Wilson, J.A. Valerio and S. Gottesfeld, *Electrochim. Acta* **40** (1995) 355.
11. M.S. Wilson and S. Gottesfeld, *J. Appl. Electrochem.* **22** (1992) 1.
12. C. Calmon and H. Gold, 'Ion Exchange for Pollution Control' (CRC Press Inc, 1979, Vol. 1, pp. 176–181.
13. G.C. Cushnie and W. Anderson, Removal of metal cations in chromium plating solution. In *Proceedings of AESF/EPA Hard Chromium Plating Workshop*, Orlando, FL, 1989, pp. 21–27.
14. A.F. Clifford, 'Inorganic Chemistry of Qualitative Analysis', 2nd edn (Prentice-Hall, Englewood Cliffs, NJ, 1961).
15. M. Pourbaix, 'Atlas of Electrochemical Equilibria in Aqueous Solutions' (NACE, Houston, TX, 1974).
16. M. Watanabe and S. Saegusa, *J. Electroanal. Chem.* **271** (1989) 213.
17. S. Supramaniam and M. Sanjeev, *J. Electroanal. Chem.* **357** (1993) 201.
18. D.G. Kleinbaum, L.L. Kupper and K.E. Muller, 'Applied Regression Analysis and Other Multivariable Methods' (Duxbury Press, Wadsworth Co, Belmont, CA, 1978).
19. J. Newman, 'Electrochemical Systems' 2nd edn (Prentice Hall, NJ, 1991).